Fault Diagnosis of Time-Varying Parameter Systems With Application in MEMS LCRs

Afshin Izadian, Pardis Khayyer, and Parviz Famouri, *Senior Member, IEEE*

***Abstract*—Multiple-model adaptive estimation (MMAE) is a well-known technique used for model matching of deterministic parameter systems. This technique can be used in fault diagnosis by allocating a model to each type of fault. In each contingency, the model that represents the behavior of the actual system can indicate the type of fault occurrence. Kalman filters are generally used in modeling and residual-signal generation of time-invariant systems. Slowly time-varying parameter systems, however, require a system identification unit in addition to the model-matching core. This paper utilizes the least square forgetting-factor technique in parameter identification of slowly time-varying systems and combines it with MMAE for fault-diagnosis applications in microelectromechanical-systems (MEMS) lateral comb resonators (LCRs). Prescheduled faults were designed for simulations and experimentally examined in real-time implementations of estimation-based diagnosis technique for two fabricated MEMS LCRs. It is shown that the application of a system identification unit significantly increases the performance of the fault diagnosis in MEMS devices.**

***Index Terms*—Fault diagnosis, forgetting factor, microelectromechanical-systems (MEMS) lateral comb resonators (LCRs), multiple-model adaptive estimation (MMAE).**

I. Introduction

MULTIPLE-MODEL adaptive estimators (MMAEs) generally reveal the behavior of linear time-invariant systems by weighting the output of several models simultaneously according to input–output measurements and evaluating their residual signals. Kalman filters are conventionally used in modeling of time-invariant systems under different conditions. The history of output variations (in the actual system) also has a considerable effect on the performance of the model-matching core. In uncertain or time-varying parameter systems, techniques other than Kalman filters are required for model matching and weight allocations. The effect of recent data (variations) must be controlled in order to accurately identify the parameters of systems and result in high-performance model-matching units.

Some model-matching units introduce local states for local models and accept possible transitions [1]. Graphical structures are also applied to describe the transitions among models which require *a priori* knowledge of the system [2]. Operating systems, however, are modeled by different techniques such as piecewise modeling, spline, and statistical approaches as well as fuzzy and neural networks [3]–[7].

In slowly time-varying parameter systems, in addition to the model-matching core, a separate unit is needed to identify the model parameters and its variations. The parameter identification unit may be replaced with Kalman filter banks in conventional MMAE configurations. Like Kalman filters, the identification unit must factor in the noise in the system and compute the output deviations to generate residual signals. Since the history of the variations (i.e., the output of the actual system) affects the performance of model matching, forgetting-factor recursive least square (FFRLS) is applied to weight the recent data appropriately and to identify the parameters of the system accurately [8]. Thus, MMAE applied in time-varying parameter systems will contain several system identification units and one model-matching core.

In this paper, the main purpose is to design a system for fault diagnosis of microelectromechanical systems (MEMS) devices. Since the parameters of MEMS slowly vary over time, the forgetting-factor technique is used. The system identification unit (in the form of self-tuning blocks) and model-matching core are combined for a second-order mass–spring–damper system (model of MEMS). FFRLS is usually used for single-input–single-output systems; however, for multiple-input and multiple-output systems, a proper number of identifiers can estimate the whole system parameters. The algorithm is implemented experimentally for the fault diagnosis of two fabricated lateral comb resonators (LCRs) and for intentionally simulated faults during the operation. The results of the system identification and fault diagnosis are compared with those obtained from Kalman filters without the application of a system identification unit.

II. System Modeling

Different contingencies of the actual system are modeled in the form of separate submodels. The actual system, which can also be influenced by noise and parameter variations, is expressed in state-space form as

$$\begin{aligned} x(t_i) &= \Phi x(t_{i-1}) + \Gamma u(t_{i-1}) + Gw(t_i) \\ z(t_i) &= Hx(t_i) + v(t_i) \end{aligned} \tag{1}$$

Manuscript received April 10, 2008; revised October 24, 2008. First published December 2, 2008; current version published April 1, 2009. This work was supported in part by the National Aeronautics and Space Administration and in part by the National Science Foundation.

A. Izadian and P. Khayyer are with Cummins Inc., Columbus, IN 47203 USA (e-mail: Afshin.izadian@cummins.com; khayyer@ieee.org).

P. Famouri is with the Lane Department of Computer Science and Electrical Engineering, West Virginia University, Morgantown, WV 26506 USA (e-mail: Pfamouri@wvu.edu).

Color versions of one or more of the figures in this paper are available online at http://ieeexplore.ieee.org.

Digital Object Identifier 10.1109/TIE.2008.2010095

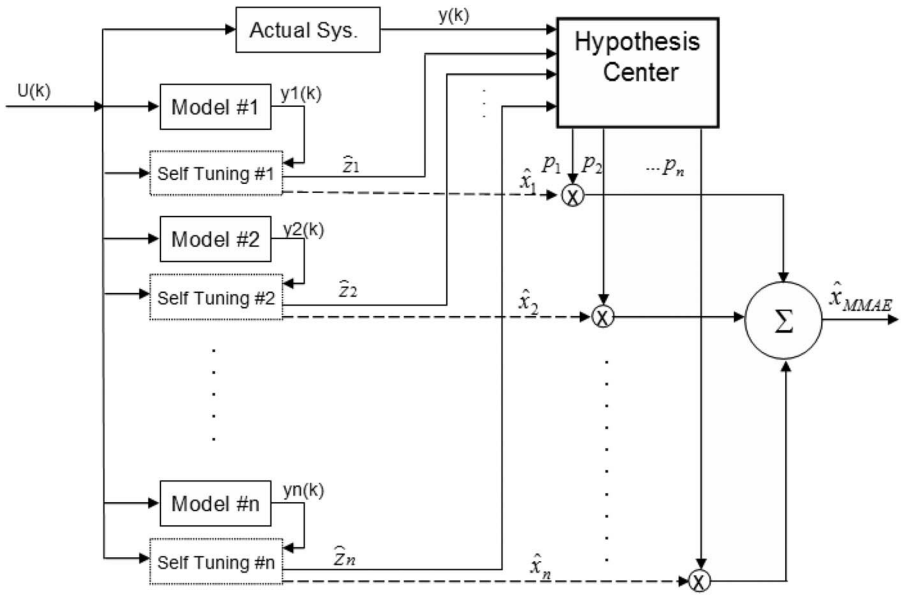

Fig. 1. Multiple-model adaptive estimator using self-tuning banks.

where $x(t_i)$ is the state-space variable at time t_i, Φ is the system matrix with slowly varying parameters, Γ is the input matrix, u is the input vector, G is the noise input matrix, and z is the output measurement vector of the model. H is the output matrix, $w(t_i)$ is a zero-mean discrete-time white noise in the input, and $v(t_i)$ is a zero-mean discrete-time white measurement noise in the output of the system. The variances of system (Q) and measurement noise (R) are independent values, which might change in each model, and are defined as

$$E\left\{w(t_i)w^{\mathrm{T}}(t_j)\right\} = \begin{cases} Q, & t_i = t_j \\ 0, & t_i \neq t_j \end{cases} \tag{2}$$

$$E\left\{v(t_i)v^{\mathrm{T}}(t_j)\right\} = \begin{cases} R, & t_i = t_j \\ 0, & t_i \neq t_j. \end{cases} \tag{3}$$

The parameters of model (1) can be adjusted according to different conditions and parameter variation. For instance, an estimation of the kth subsystem is expressed as

$$\begin{aligned} \hat{x}_k(t_i) &= \hat{\Phi}_k \hat{x}_k(t_{i-1}) + \hat{\Gamma}_k u(t_{i-1}) \\ \hat{z}_k(t_i) &= \hat{H}_k \hat{x}_k(t_i) \end{aligned} \tag{4}$$

where $(\hat{})$ sign indicates the matrices and state variables of estimated values. Submodels, shown in Fig. 1, are connected in parallel with self-tuning banks (containing the system-identification algorithm); therefore, each submodel is represented separately in the form of (4). In other words, submodels are specific representations of the system's behavior under different conditions. Parameter-identification blocks in the form of self-tuning banks can also estimate the output of these subsystems. Estimated output signals, when compared to the output of the actual system, generate residual signals and are used to compute the weights applied to the estimated state-space variables.

III. Theory Development

A. Estimator Blocks (Self-Tuning)

The main purpose of a self-tuning unit is to estimate the parameters and output of a system. In slowly varying parameter systems, RLS technique is applied. A forgetting factor is utilized where the history of variation affects the performance of estimation.

Consider an autoregressive-moving-average system representing the kth subsystem which is expressed as

$$\begin{aligned} z_k(t_{i+1}) = b_0 u(t_i) + \cdots + b_m u(t_{i-m}) \\ -a_1 z_k(t_i) - \cdots - a_n z_k(t_{i-n+1}) \end{aligned} \tag{5}$$

where a_i's are the coefficients of the denominator polynomial (input polynomial), b_i's are the coefficients of the numerator (output polynomial) of the system, and u, z_k are the input and output signals of the k subsystem, respectively. The unknown parameter values of the system are listed in a vector as

$$\theta^{\mathrm{T}} = [b_0 b_1, \ldots, b_m, a_1 a_2, \ldots, a_n]. \tag{6}$$

The size of the unknown vector is $l = m + n + 1$, where $m + 1, n$ represent the order of the numerator and denominator polynomials, respectively. The model's input–output sets can be expressed as a regressor matrix as

$$\begin{aligned} h^{\mathrm{T}}(t_i) = [u(t_i)u(t_{i-1}), \ldots, u(t_{i-m}), -z_k(t_i), \\ -z_k(t_{i-1}), \ldots, -z_k(t_{i-n+1})]. \end{aligned} \tag{7}$$

The system can be represented in a compact form as

$$z_k(t_{i+1}) = h^{\mathrm{T}}(t_i)\theta(t_i). \tag{8}$$

The estimated output is obtained by substituting an estimate of parameter values $\hat{\theta}(t_i)$ in (8) as

$$\hat{z}_k(t_{i+1}) = h^{\mathrm{T}}(t_i)\hat{\theta}(t_i). \tag{9}$$

Estimated parameters of the system are carried out recursively, utilizing the RLS identification algorithm as [9]

$$\hat{\theta}(t_{i+1}) = \hat{\theta}(t_i) + \eta(t_i)h(t_i)\left\{1 + h^{\mathrm{T}}(t_i)\eta(t_i)h(t_i)\right\}^{-1} \times \left\{z(t_{i+1}) - h^{\mathrm{T}}(t_i)\hat{\theta}(t_i)\right\} \quad (10)$$

where $\eta(t)$ is the covariance matrix which is defined and updated as

$$\eta(t_{i+1}) = \eta(t_i) - \left\{1 + h^{\mathrm{T}}(t_i)\eta(t_i)h(t_i)\right\}^{-1} \times \left\{\eta(t_i)h(t_i)h^{\mathrm{T}}(t_i)\eta(t_i)\right\}. \quad (11)$$

Applying the FFRLS, time-varying parameters are estimated by introducing the forgetting factor λ as follows [9]:

$$\hat{\theta}(t_{i+1}) = \hat{\theta}(t_i) + \eta(t_i)h(t_i)\left\{\lambda + h^{\mathrm{T}}(t_i)\eta(t_i)h(t_i)\right\}^{-1} \times \left\{z(t_{i+1}) - h^{\mathrm{T}}(t_i)\hat{\theta}(t_i)\right\}. \quad (12)$$

Applying the forgetting factor to the covariance matrix $\eta(t)$ gives

$$\eta(t_{i+1}) = \frac{1}{\lambda}\Big[\eta(t_i) - \left\{\lambda + h^{\mathrm{T}}(t_i)\eta(t_i)h(t_i)\right\}^{-1} \times \left\{\eta(t_i)h(t_i)h^{\mathrm{T}}(t_i)\eta(t_i)\right\}\Big] \quad (13)$$

where $0 < \lambda < 1$ is the forgetting factor.

Residual signals, which are defined as differences between the actual system's output and those of submodels, are obtained by

$$r_k(t_i) = y(t_i) - \hat{H}_k\hat{x}_k(t_i). \quad (14)$$

B. MMAE (Model Matching)

The hypothesis-testing algorithm (the weight-allocation unit) continuously monitors the residual-signal variations. If the estimated outputs in any of the subsystems match the output of the actual system, the mean value of that residual signal becomes zero. In this case, the covariance matrix of that system can be computed as [10]

$$\psi_k = \hat{H}_k P_k \hat{H}_k^{\mathrm{T}} \quad (15)$$

where P_k is recursively updated by

$$P_k(t_{i+1}) = \hat{G}_k Q \hat{G}_k^{\mathrm{T}} + \hat{\Phi}_k P_k(t_i)\hat{\Phi}_k^{\mathrm{T}} - \hat{\Phi}_k P_k(t_i)\hat{H}_k \times \left[R + \hat{H}_k P_k(t_i)\hat{H}_k^{\mathrm{T}}\right]^{-1} \hat{H}_k P_k(t_i)\hat{\Phi}_k^{\mathrm{T}}. \quad (16)$$

The conditional probability density function for the kth subsystem, when considering the measurement signal's history, $Z(t_{i-1}) = [z^{\mathrm{T}}(t_1), \ldots, z^{\mathrm{T}}(t_{i-1})]$, is expressed as [10]

$$f_{\hat{z}(t_i)|h,\hat{Z}(t_{i-1})}(\hat{z}_i|h_k, \hat{Z}_{i-1}) = \beta_k \exp\{\bullet\} \quad (17)$$

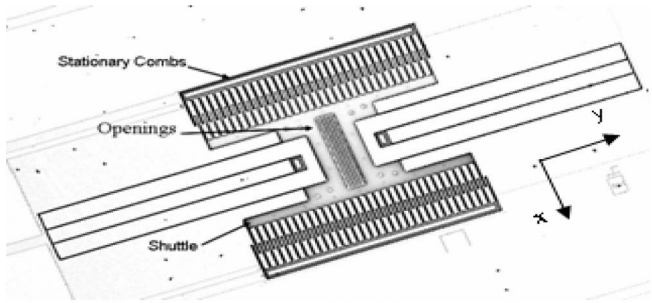

(a)

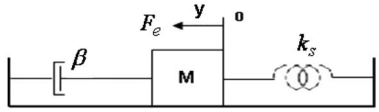

(b)

Fig. 2. (a) LCR manufactured by WVU. (b) Mass–spring–damper schematic model of LCR.

with

$$\beta_k = \frac{1}{(2\pi)^{l/2}|\psi_k|^{l/2}} \quad (18)$$

where l is the size of the output matrix and

$$\{\bullet\} = \left\{-\frac{1}{2}r_k^{\mathrm{T}}(t_i)\psi_k^{-1}r_k(t_i)\right\}. \quad (19)$$

The conditional probability (Pr) values for the kth system is defined as

$$p_k(t_i) = \Pr\left\{h = h_k|\hat{Z}(t_i) = \hat{Z}_i\right\}. \quad (20)$$

This value can also be computed by

$$p_k(t_i) = \frac{f_{\hat{z}(t_i)|h,\hat{Z}(t_{i-1})}(\hat{z}_i|h_k, \hat{Z}_{i-1}) \cdot p_k(t_{i-1})}{\sum_{j=1}^{K} f_{\hat{z}(t_i)|h,\hat{Z}(t_{i-1})}(\hat{z}_i|h_j, \hat{Z}_{i-1}) \cdot p_j(t_{i-1})}. \quad (21)$$

The conditional probability functions make use of an *a priori* sample to compute the current values and are normalized over the sum of conditional probabilities in all subsystems [10]. The largest of all the probability values, allocated to a particular system, is an indicator of validity of that subsystem. In case the probability values change rapidly and make the output of the subsystem unpredictable, the output should be compared with a threshold [10] (for more information on the computations of the threshold, please see [11]).

IV. MEMS LCRs

In this section, the MMAE unit, equipped with self-tuning banks, is applied for fault diagnosis of MEMS LCRs. The structure of these devices and their governing equations has been investigated in [12]–[21].

In this section, an LCR is briefly introduced for the convenience of readers. A typical LCR consists of a moving stage (also known as a shuttle), stationary combs, and suspension springs located on the sides [Fig. 2(a)]. The LCR can be

TABLE I
FAULT SCENARIO AND PARAMETER VARIATIONS

Contingencies	1	2	3	4	5	6	7
Samples	0-2k	2k-3k	3k-4k	4k-5k	5k-6k	6k-7k	7k-end
Parameter Variation	M,B, K Healthy	+5% M B, K	+10%M B, K	+5% K M, B	+10% K M, B	+30% B M, K	M, B, K Healthy

modeled as a mass–spring–damper system [Fig. 2(b)] in a second-order differential equation as

$$F_e = m\ddot{y} + \beta\dot{y} + 2k_s y \tag{22}$$

where m is the mass of the center comb (shuttle), y is the displacement, k_s is the spring constant on one side, and β is the damping coefficient. Considering the parameter uncertainties and the effect of fault on the parameter variations of the device, a discrete state-space representation of an LCR is

$$x(q+1) = \Phi x(q) + \Gamma u(q) \tag{23}$$

where q is the time step. The main purpose is to track the parameter variations and to find an effective way of monitoring the behavioral changes in MEMS.

V. FAULT DIAGNOSIS OF MEMS

A. Diagnosis and Simulation

In order to simulate the fault-diagnosis technique in MEMS devices, a fault scenario containing different parameter variations was designed. The fault scenario contained a sequence of events as follows (also see Table I):

1) healthy (normal) operation for 2000 samples;
2) $+5\%$ mass variation for 1000 samples;
3) $+10\%$ mass variation for 1000 samples;
4) $+5\%$ spring-constant variation for 1000 samples;
5) $+10\%$ spring-constant variation for 1000 samples;
6) $+30\%$ change in damping coefficient for 1000 samples;
7) return to normal condition after 2000 samples.

These series of events occur consecutively and cover common types of parameter variations in microsystems.

The FFRLS estimation algorithm was initialized by $P = 1e8^* I_{4\times 4}$ with forgetting factor of $\lambda = 0.86$ (which is obtained by trial and error). Fig. 3 shows the diagnostic performance in each step of the fault scenario by allocating a probability value to each of the models. Higher probability values (i.e., closer to one) indicate a match of the system to that particular subsystem. For instance, in step 1) (from the scenario), the system operated under normal conditions, and simulations confirm this fact by allocating a high probability to the subsystem number one. As shown, other probability values are negligible.

The speed of transitions from one step to another and probability variations during the operation of a model are all indicative of diagnostic performance. As Fig. 3 shows, there is no significant delay observed during transitions, and the probability is smooth in operation of the model.

Initializing the system identification at different forgetting factors results in different diagnosis profiles. At higher forgetting factors, distortions were observed in transitions among models. As shown in Fig. 4, at $\lambda = 0.9$, the diagnosis profile shows distortion in transition from steps 2 to 3 of the fault scenario ($+5\%$ and $+10\%$ mass-change cases). However, the self-tuning banks could estimate the parameters given the existence of noise in the system, and the fault-diagnosis algorithm could identify the rest of the variations properly with a short transition time. There was no significant delay observed in transitions among other steps of the fault scenario.

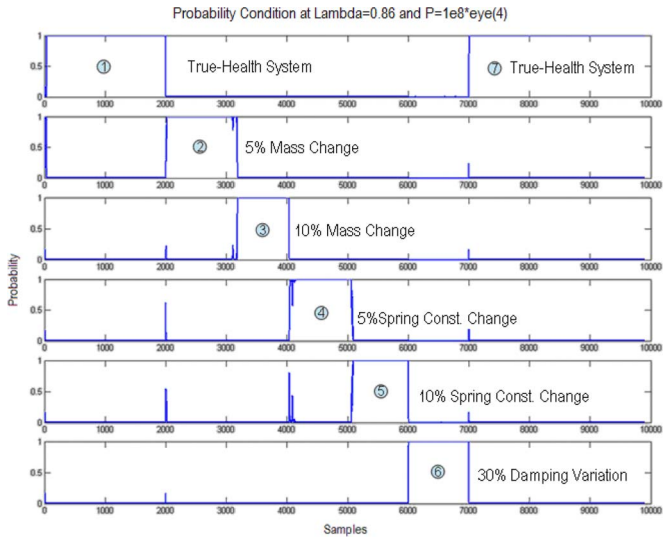

Fig. 3. Conditional probability values according to the fault scenario with FFRLS at $\lambda = 0.86$, $P = 1e8 * I$.

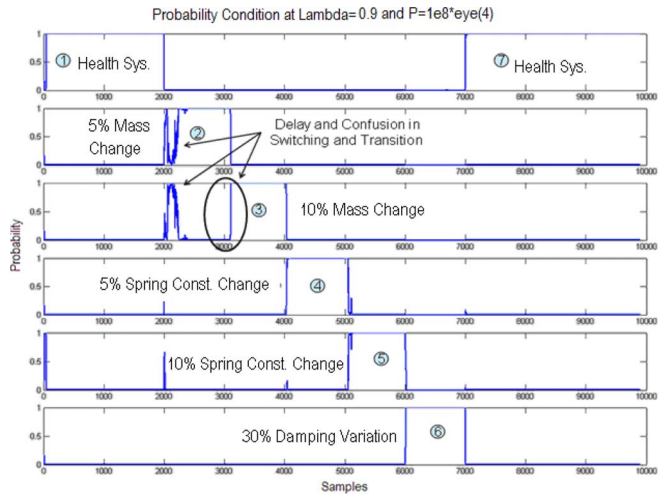

Fig. 4. Conditional probability values according to the fault scenario with FFRLS at $\lambda = 0.9$, $P = 1e8 * I$.

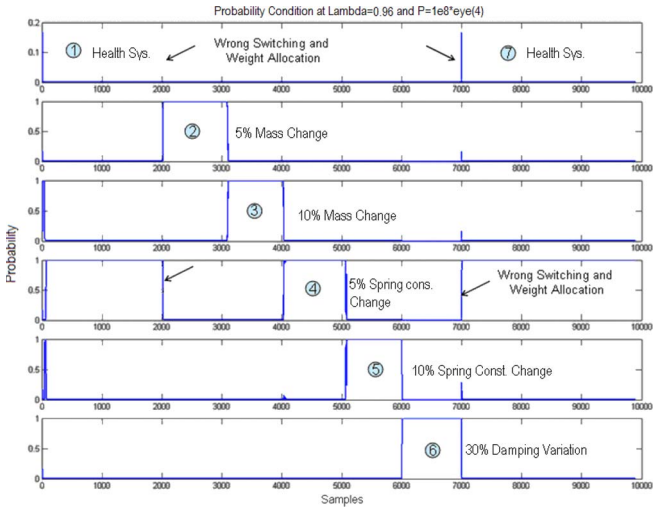

Fig. 5. Conditional probability values according to the fault scenario with FFRLS at $\lambda = 0.98$, $P = 1e8 * I$.

TABLE II
ESTIMATED PARAMETERS OF TWO FABRICATED SYSTEMS

	Mass (kg)	Ks (N/m)	Beta (N/(m/s))
System #1	2.3856e-10	0.0193	7.563e-7
System #2	2.2429e-10	0.0448	1.385e-6

Increasing the forgetting factor to higher values resulted in a short history of data for the conditional probability density functions and initiated delays in weight computations.

As shown in Fig. 5, the fault diagnosis was completely dysfunctional at $\lambda = 0.98$, wherein wrong diagnosis was observed in steps 1) and 4) and steps 6) and 7).

Taking into account the level of noise in the system and the rate of parameter variations, satisfactory transitions and precise parameter estimation were observed in the range of $0.86 < \lambda < 0.9$. Values outside of this boundary changed the history of data and caused distortions in transitions. Self-tuning banks could successfully estimate the subsystem parameters and output signals at a suitable forgetting-factor value and result in a robust decision-making unit under various conditions.

B. Diagnosis and Experiment

The parameter-identification technique using FFRLS was used to experimentally identify the parameters of two fabricated LCRs. Parameters of these devices were intentionally designed differently in order to test the abilities of the model-matching core equipped with identification units.

In the design of the LCR devices, spring constants were different; however, after fabrication, due to imperfect manufacturing steps, there was also a variation observed between the damping coefficients of the devices. The parameters of these fabricated devices are listed in Table II, which indicate an almost identical mass, 130% variation in spring constant, and 83% variation in damping coefficient.

The LCR devices were sequentially excited by the same waveform, and their outputs were recorded separately. These signals (outputs) were joined together to form a fault in the system. The fault was scheduled to occur at the 1886th sample point in the resulting output. Interested readers on optical methods and data recovery involved in the displacement recording are referred to [22]–[25].

TABLE III
SELF-TUNING SYSTEM IDENTIFICATION RESULTS FOR LCR SYSTEMS 1 AND 2 USING FORGETTING FACTOR $\lambda = 0.8$

System 1	$\hat{x}(q+1) = \begin{bmatrix} 1.9934 & -0.9935 \\ 1.0000 & 0 \end{bmatrix} \hat{x}(q) + \begin{bmatrix} 0.3052e-4 \\ 0 \end{bmatrix} u(q)$
System 2	$\hat{x}(q+1) = \begin{bmatrix} 1.9882 & -0.4944 \\ 2.0000 & 0 \end{bmatrix} \hat{x}(q) + \begin{bmatrix} 0.3052e-4 \\ 0 \end{bmatrix} u(q)$

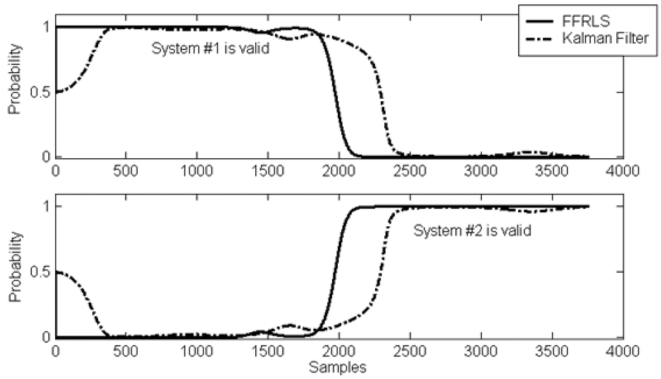

Fig. 6. Weight allocation and conditional probability densities from test of two fabricated LCRs. Switching from systems 1 to 2 is shown at $\lambda = 0.8$.

Parameter identification units revealed two sets of discrete state-space equations for two fabricated LCRs at $\lambda = 0.8$ (see Table III). Parameter identification shows the same diagonal values in the system matrix, although the effects of parameter variation are better observed in the off-diagonal values of this matrix.

Applying MMAE technique and self-tuning estimators together resulted in the weight allocations and probability computations shown in Fig. 6. As the figure shows, the highest weight was allocated to system 1 in the early steps of the first part of the test, which means that the actual system was similar to subsystem 1. At the fault point (sample 1886), the weight began shifting toward system 2, and the transition was completed in a short time. There was no significant variation observed in the calculated weights before the moment of fault in the first part. After the fault, system 2 had higher weight and probability values, demonstrating the operation under fault. Thus, MMAE and self-tuning together could successfully identify the multiple parameter variations resulting from a fault in the system.

Fig. 6 also shows the benefit of applying a system identification unit along with the model-recognition core. As shown, Kalman filters could recognize the fault in the system; however, the diagnosis operation contained a long delay at the start point and at the point of fault. Therefore, it is clear that application of parameter identification units in fault diagnosis improves the performance of fault diagnosis in MMAE technique.

VI. CONCLUSION

The application of MMAE technique in time-varying parameter systems was illustrated in this paper. The overall system consisted of a model-matching core and several estimation

units. The model-matching core weighted the output of subsystems to find the subsystem that best represented the actual system's behavior. History of output variation directly influenced the diagnostic performance; thus, forgetting-factor parameter-estimation technique was applied to control and weigh recent data. Application of parameter estimators in MMAE was experimentally verified by fault diagnosis of fabricated MEMS LCRs. The performance of fault diagnosis was significantly improved by application of parameter estimation units along with a model-matching core.

ACKNOWLEDGMENT

The authors would like to thank Dr. L. Wang and Dr. S. Almashat for their time and helpful comments.

REFERENCES

[1] B. Kuipers and K. Astrom, "The composition and validation of heterogeneous control laws," *Automatica*, vol. 30, no. 2, pp. 233–249, Feb. 1994.
[2] J. Whittaker, *Graphical Models in Applied Multivariate Statistics*. Hoboken, NJ: Wiley, 1991.
[3] R. E. Bellman, *Adaptive Control Processes*. Princeton, NJ: Princeton Univ. Press, 1990.
[4] V. I. Opoitsev, "Identification of static plants by means of piecewise linear functions," *Autom. Remote Control*, vol. 31, pp. 809–815.
[5] J. E. Stromberg, F. Gustafsson, and L. Ljung, "Trees as black box model structures for dynamical systems," in *Proc. Eur. Control Conf.*, Grenoble, France, 1991, pp. 1175–1180. [Online]. Available: https://eidr.wvu.edu/etd/documentdata.eTD?documentid=3711
[6] G. Wahba, *Spline Models for Observational Data (Regional Conference Series in Applied Mathematics)*. Philadelphia, PA: SIAM, 1990. [Online]. Available: http://www.ec-securehost.com/SIAM/CB59.html
[7] M. J. D. Powell, *Radial Basis Functions for Multivariable Interpolation: A Review in Algorithms for Approximation*. Oxford, U.K.: Clarendon, pp. 143–167.
[8] W. Zhuang, *RLS Algorithm With Variable Forgetting Factor for Decision Feedback Equalizer Over Time-Variant Fading Channels*, 1999. [Online]. Available: http://www.cwc.uwaterloo.ca/tech_reports/zhuang3.pdf
[9] P. E. Wellstead and M. B. Zarrop, *Self-Tuning Systems Control and Signal Processing*. Hoboken, NJ: Wiley, 1999.
[10] P. Hanlon and P. S. Maybeck, "Multiple-model adaptive estimation using a residual correlation Kalman filter bank," *IEEE Trans. Aerosp. Electron. Syst.*, vol. 36, no. 2, pp. 393–406, Apr. 2000.
[11] S. L. Campbell and R. Nikoukhah, *Auxiliary Signal Design for Failure Detection*. Princeton, NJ: Princeton Univ. Press, 2004.
[12] A. Izadian and P. Famouri, "Reliability enhancement of MEMS lateral comb resonators under fault conditions," *IEEE Trans. Control Syst. Technol.*, vol. 16, no. 4, pp. 726–734, Jul. 2008.
[13] J. M. Dawson, L. Wang, J. Chen, P. Famouri, and L. A. Hornak, "MEMS feedback control using through-wafer optical device monitoring," in *Proc. SPIE*, vol. 4178, pp. 221–231.
[14] A. Izadian, L. Hornak, and P. Famouri, "Adaptive control of MEMS devices," in *Proc. Int. Conf. ISC*, Honolulu, HI, Aug. 14–16, 2006, pp. 107–112.
[15] A. M. Shkel, R. Horowitz, A. A. Seshia, S. Park, and R. T. Howe, "Dynamics and control of micromachined gyroscopes," in *Proc. Amer. Control Conf.*, San Diego, CA, 1999, pp. 2119–2124.
[16] R. Horowitz, P. Cheung, and R. T. Howe, *Position Sensing and Control of Electrostatically Driven Polysilicon Micro Actuator*, pp. P-1–P-2.
[17] G. K. Fedder and R. T. Howe, "Multimode digital control of a suspended polysilicon microstructure," *J. Microelectromech. Syst.*, vol. 5, no. 4, pp. 283–297, Dec. 1996.
[18] W. T. Tang, M. G. Lim, and R. T. Howe, "Electrostatic comb drive levitation and control method," *J. Microelectromech. Syst.*, vol. 1, no. 4, pp. 170–178, Dec. 1992.
[19] S. Bhansali, A. L. Zhang, R. B. Zmood, P. E. Jones, and K. Sood, "Prototype feedback-controlled bi-directional actuation system for MEMS applications," *J. Microelectromech. Syst.*, vol. 9, no. 2, pp. 245–251, Jun. 2000.
[20] Y. Li and R. Horowitz, "Active suspension vibration control with dual stage actuators in hard disk drives," in *Proc. Amer. Control Conf.*, Arlington, VA, Jun. 2001, pp. 2786–2791.
[21] S. Pannu, C. Chang, R. S. Muller, and A. P. Pisano, "Closed-loop feedback-control system for improved tracking in magnetically actuated micromirrors," in *Proc. IEEE/LEOS Int. Conf. Opt. MEMS*, Kauai, HI, Aug. 21–24, 2000, pp. 107–108.
[22] L. Wang, "Modeling and real-time feedback control of MEMS device," Ph.D. dissertation, Comput. Sci. Elect. Eng. Dept., West Virginia Univ., Morgantown, WV, 2005.
[23] L. Wang, J. M. Dawson, L. A. Hornak, P. Famouri, and R. Ghaffarian, "Real time transitional control of a MEMS comb resonator," *IEEE Trans. Aerosp. Electron. Syst.*, vol. 40, no. 2, pp. 567–575, Apr. 2004.
[24] A. Izadian, l. Hornak, and P. Famouri, "Structure rotation and pull-in voltage control of MEMS lateral comb resonators under fault conditions," *IEEE Trans. Control Syst. Technol.*, vol. 17, no. 1, pp. 51–59, Jan. 2009.
[25] J. M. Dawson, J. Chen, K. S. Brown, P. Famouri, and L. A. Hornak, "Through-wafer optical probe characterization for microelectromechanical systems positional state monitoring and feedback control," *Opt. Eng.*, vol. 39, no. 12, pp. 3239–3246, Dec. 2000.

Afshin Izadian received the M.S. degree in electrical engineering from Iran University of Science and Technology, Tehran, Iran, in 2001, and the Ph.D. degree (with the highest rank as an outstanding student) in electrical engineering from West Virginia University, Morgantown, in 2008.

From 2001 to 2004, he was an Electrical Engineer with Moshanir Power Consultant Company, Tehran. He is currently with Cummins Inc., Columbus, IN. His research interests include adaptive control, fault diagnosis, electric machines, and electric vehicles.

Dr. Izadian is a member of Eta Kappa Nu and Tau Beta Pi.

Pardis Khayyer received the B.S. degree in electrical engineering from Shiraz University, Shiraz, Iran, in 2005, and the M.S. degree in electrical engineering from West Virginia University, Morgantown, in 2008.

She was a Graduate Research Assistant with the Electromechanical Systems Laboratory, West Virginia University, and has co-op experience with EPM Inc., Framingham, MA. She is currently a Controls Engineer with Cummins Inc., Columbus, IN. Her research interests include control and fault diagnosis of electromechanical systems, vehicle propulsion systems, hybrid fuel-cell vehicles, and control and power management of the vehicles.

Prof. Khayyer is a member of Eta Kappa Nu and Tau Beta Pi.

Parviz Famouri (SM'86) received the B.S. degree in applied mathematics from Kentucky State University, Frankfort, in 1981, and the B.S., M.S., and Ph.D. degrees in electrical engineering from the University of Kentucky, Lexington, in 1982, 1986, and 1990, respectively.

He is currently a Professor and the Associate Chair for graduate studies with the Lane Department of Computer Science and Electrical Engineering, West Virginia University, Morgantown. He is the author of over 100 papers in the fields of electromechanics and control. His primary interests include design, analysis, modeling, and control of electromechanical systems, microelectromechanical systems, and nano electro mechanical systems (NEMS). He has served as Principle Investigator on projects for the National Science Foundation, the Department of Defense, the Department of Energy, and NASA.